International Journal of Microwave and Wireless Technologies

cambridge.org/mrf

Mutual-coupling reduction in triple-band MIMO antennas for WLAN using CSRRs

Vahid Najafy[1] and Mohammad Bemani[2]

[1]Department of Electrical and Computer Engineering, University of Tarbiat Modares, Tehran, Iran and
[2]Department of Electrical and Computer Engineering, University of Tabriz, Tabriz, Iran

Research Paper

Cite this article: Najafy V, Bemani M (2020). Mutual-coupling reduction in triple-band MIMO antennas for WLAN using CSRRs. *International Journal of Microwave and Wireless Technologies* **12**, 762–768. https://doi.org/10.1017/S1759078720000215

Received: 28 November 2019
Revised: 23 February 2020
Accepted: 25 February 2020
First published online: 19 March 2020

Key words:
Metamaterial; multiple-input multiple-output (MIMO); mutual coupling; triple-band complementary split-ring resonator

Author for correspondence:
Mohammad Bemani,
E-mail: bemani@tabrizu.ac.ir

Abstract

For the requirements of low mutual-coupling MIMO antennas for WLAN, a new complementary split-ring resonator (CSRR) unit cell is introduced in this paper. A microstrip-fed Vivaldi antenna array is designed for WLAN applications, where compact triple-band gap-complementary split-ring resonator unit cells are loaded between two antennas to examine the effect of unit cells on the rate of mutual-coupling reduction. By inserting the CSRR, the final design offered an improvement in decoupling by 8.5, 10.5, and 18 dB at 3.65, 4.9, and 5.8 GHz, respectively, compared with the reference antenna. By suppressing surface waves, antenna gain and front-to-back ratio are improved.

Introduction

Nowadays, having wireless communication with a high capacity and low error rate is critical. Also, multiple-input and multiple-output (MIMO) systems are appropriate options for achieving these goals. One of the main parameters in these systems is the availability of multiple independent channels; that way, when the channel correlation is maximized, MIMO systems will not be different than single-channel communication systems [1]. Mutual coupling between the antennas is one of the most important factors affecting the correlation. An increase in the distance between the antennas helps reduce its effects; however, the advancement of technology and the need for small telecommunication devices, especially in the fifth generation multiband systems [2], have prompted researchers to study how to reduce mutual coupling [3]. One of the main sources of mutual coupling is the surface wave. Control and reduction of the surface wave are related to the performance of an MIMO system [4]. Thus, according to the sources of mutual coupling and also trying to constrain the size, the coupling between the antenna elements increases in various frequency bands in a multi-band MIMO system. Therefore, research on the decoupling of multi-band antennas is important.

In recent years, various techniques including defected ground structure [5], optimizing array configuration [1], frequency selective surface, electromagnetic band gap (EBG) [4, 6–9], and metamaterials [10–14] have been suggested. In [15], through dual-band enhancing isolation by providing a new dual-band, EBG was achieved; nevertheless, conventional models of EBG structures gave their place to uniplanar models such as those in [16, 17] due to electrical losses caused by the vias and owing to more difficulty in construction. In [17], the small size of a proposed uniplanar EBG reduced the distance between two antennas and decreased mutual coupling 19 and 11 dB in the *E*-plane and *H*-plane at 5.8 GHz. One of the practical ways of enhancing isolation is a 3D structure, which has been used in [3, 13, 18–21]. One can say that 3D-dimensionality of the structure and egress final antenna from the planar state are the most important disadvantages of the mentioned studies. Complementary split-ring resonators (CSRRs) constitute another method of reducing coupling, which is a simple way to achieve a −10 dB reduction in the mutual coupling at a single band [22]. Overall, there is a gap in finding a simple method which is also expandable in multi-band applications.

In this paper, a compact triple-band gap-complementary split-ring resonator (CTBG-CSRR) unit cell has been presented, which is loaded between two microstrip-fed Vivaldi antennas to reduce mutual coupling in the triple band for WLAN applications. Because final size of the unit cell is compact, the edge to edge distance of the two antennas is close, which also improves the front-to-back ratio of Vivaldi MIMO antennas. This work is structured as follows: section "CTBG-CSRR design" presents a proposed CTBG-CSRR prototype and characterization, along with the dispersion diagram which is compared with the conventional CSRR model, and to ensure the proper function of the unit cell, it is placed in a parallel waveguide structure. In the section "Mutual coupling reduction between two microstrip-fed Vivaldi antennas," a microstrip-fed Vivaldi antenna array is designed for WLAN applications, and CTBG-CSRR unit cells are loaded between two antennas to examine the effect of unit cells on the rate of mutual-coupling reduction. Also, antenna fabrication and measurement results

CAMBRIDGE UNIVERSITY PRESS

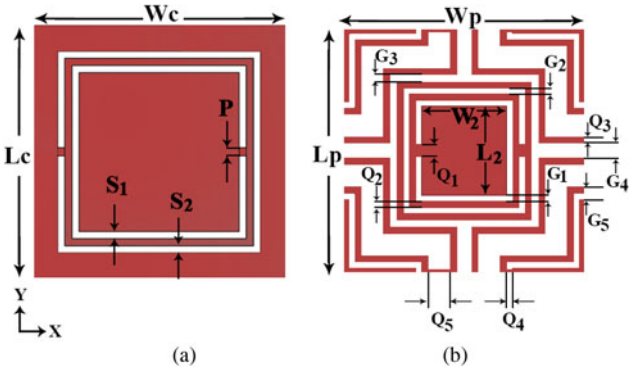

Fig. 1. (a) Conventional CSRR unit cell. Unit cell parameters: $W_c = 4$ mm, $L_c = 4$ mm, $S_1 = 1$ mm, $S_2 = 1$ mm, $P = 0.5$ mm. (b) Proposed CSRR unit cell. Unit cell parameters: $W_p = 4$ mm, $L_p = 4$ mm, $W_2 = 4$ mm, $L_2 = 4$ mm, $Q_1 = 2$ mm, $Q_2 = 2$ mm, $Q_3 = 2$ mm, $Q_4 = 2$ mm, $Q_5 = 2$ mm, $G_1 = 2$ mm, $G_2 = 2$ mm, $G_3 = 2$ mm, $G_4 = 2$ mm, $G_5 = 2$ mm.

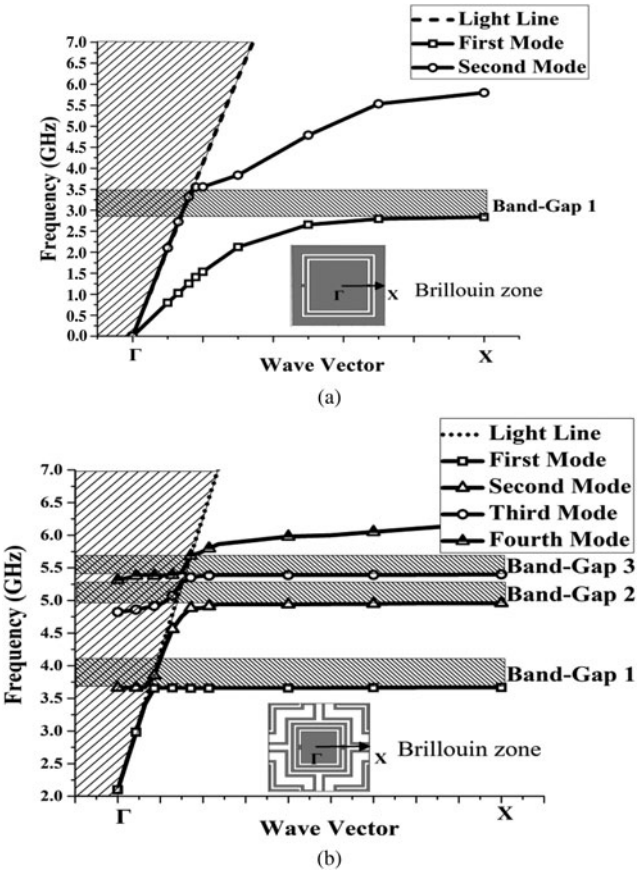

Fig. 2. Dispersion diagrams for (a) conventional and (b) proposed unit cells.

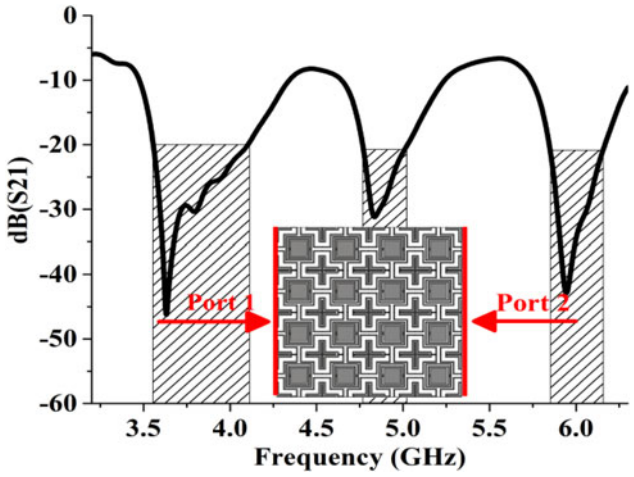

Fig. 3. Simulated S_{21} with the parallel plate waveguide method in the x-direction.

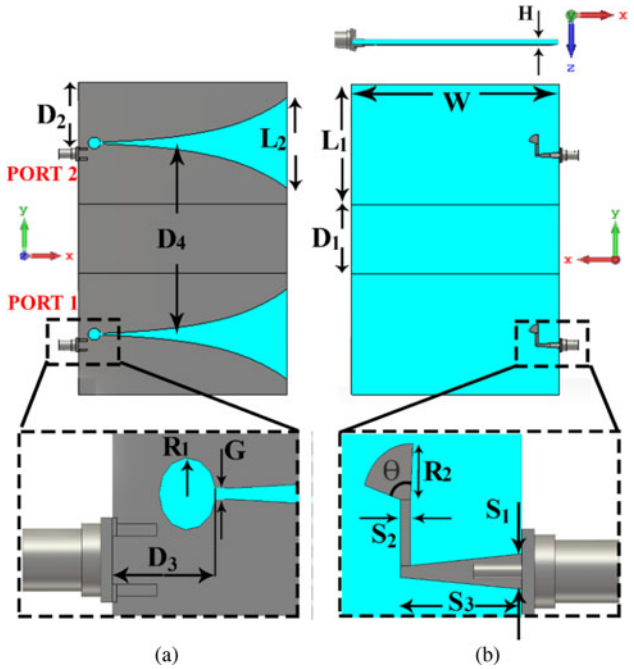

Fig. 4. Configuration of reference antenna: (a) top view and (b) bottom view: $W = 103.3$ mm , $L_1 = 60.8$ mm, $L_2 = 45.6$ mm, $S_1 = 2.9$ mm, $S_2 = 0.96$ mm, $S_3 = 11.7$ mm, $G = 0.87$ mm, $R_1 = 3$ mm, $R_2 = 0.92$ mm, $D_1 = 31.6$ mm, $D_2 = 32$ mm, $D_3 = 10.1$ mm, $D_4 = 130$ mm, $\theta = 73°$, $H = 1.6$ mm.

are outlined in this section. Finally, in the section "Conclusion," a summary together with concluding remarks and a comparison with the studies mentioned are presented.

CTBG-CSRR design

Unit cell characterization and dispersion diagram

Figure 1 displays the configurations of CTBG-CSRR unit cell. Figure 1(a) shows a customary CSRR unit cell and Fig. 1(b) exhibits the proposed unit cell. Upon placement of two cross-shaped CSRRs in all four corners of every unit conventional CSRR cell, two other frequency bands were added to it; only one-quarter of them are visible in the unit cell, which eventually causes our final model to operate as triple band. To show CTBG-CSRR stop-band characterization, the dispersion diagram of the unit cell is simulated with the eigen-mode solver using the CST Microwave Studio, where the corresponding Brillouin diagram for each unit cell is plotted along the Γ–X axis of the periodic structure. Figures 2(a) and 2(b) display the dispersion diagram of conventional and presented unit cells, respectively. As can be observed in Fig. 2(b), band-gaps which are around 3.65, 4.9, and 5.8 GHz are practical in WLAN bands.

https://doi.org/10.1017/S1759078720000215 Published online by Cambridge University Press

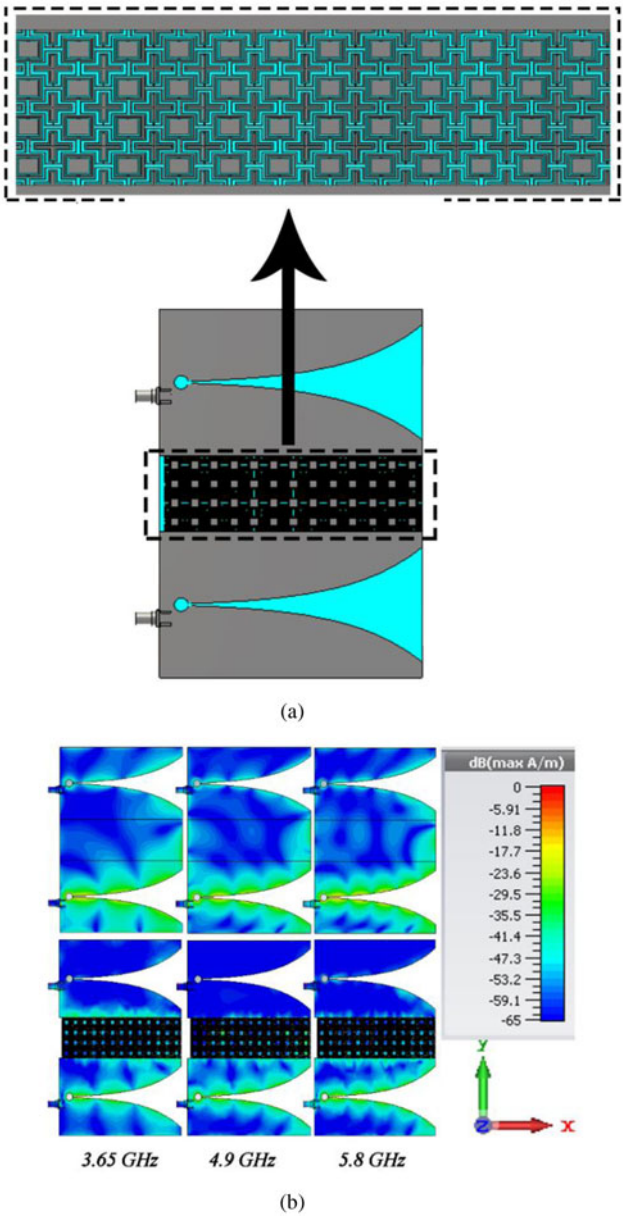

Fig. 5. (a) Proposed Vivaldi array antenna (loaded unit cell) and (b) surface current distribution at 3.65, 4.9, and 5.8 GHz in the top view of reference and proposed antennas.

Examining unit cells in parallel plate waveguide setup

To increase the simulation speed and also ensure the correct operation of the presented unit cell, parallel plate waveguide setup is used; previously, other models of transmission lines were used in [15, 19]. As illustrated in Fig. 3, 4×4 unit cells are used in the X and Y directions, and two wave ports are located in the direction of the X-axis, where the transmission coefficient between the two ports is less than 20 dB within 3.55–4.1 GHz and 4.76–5.02 GHz and 5.84–6.16 GHz. Differences in the basics of both methods (dispersion diagram and parallel plate setup) such as the limited number of unit cells used in the parallel plate setup and the lack of support for calculating losses in the eigen-mode solver method are the most important reasons for the slight difference in the operation band, especially at higher frequencies.

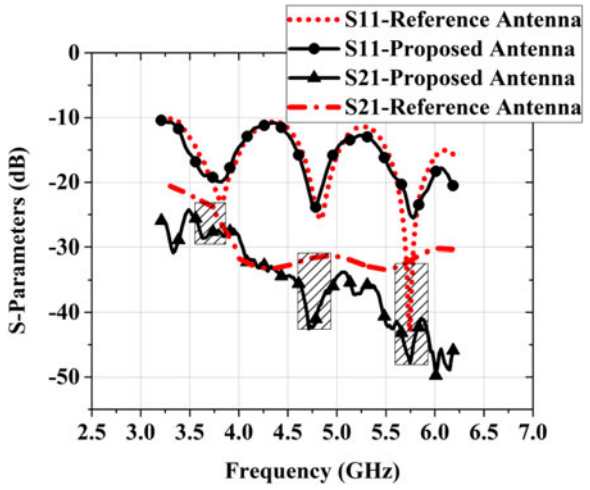

Fig. 6. Simulated transmission and reflection coefficients of the reference and proposed antenna array.

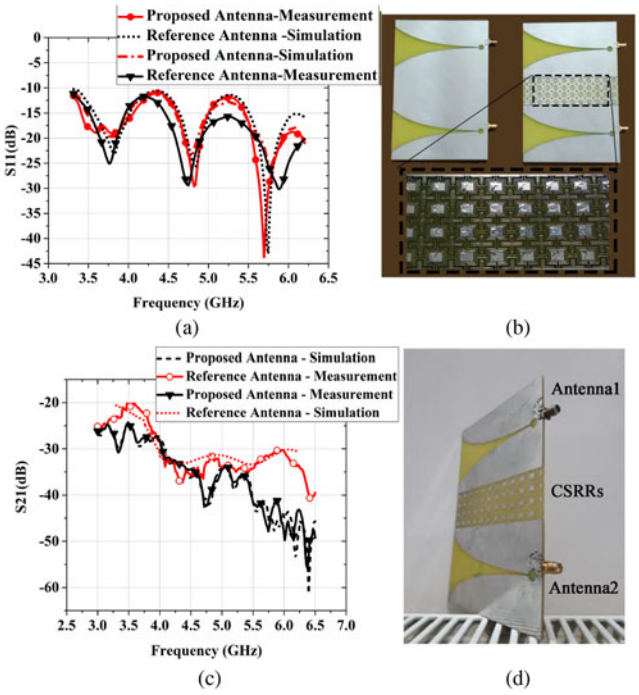

Fig. 7. Proposed Vivaldi array antenna (loaded unit cell). (a) Photograph of the fabricated antenna. (b) Measured and simulated reflection coefficient compared with the reference antenna. (c) Measured and simulated transmission coefficient compared with the reference antenna. (d) The 3D view of two antennas with CSRR.

Mutual coupling reduction between two microstrip-fed Vivaldi antennas

Microstrip-fed Vivaldi antenna array design with CTBG-CSRR loaded

A Vivaldi antenna is part of a group called traveling-wave antenna which has a wide impedance bandwidth with an end-fire radiation pattern. A microstrip-fed Vivaldi antenna is manufactured with a dielectric substrate which lies on a metal side with an exponentially tapered slot connected to a circular slot-line cavity.

https://doi.org/10.1017/S1759078720000215 Published online by Cambridge University Press

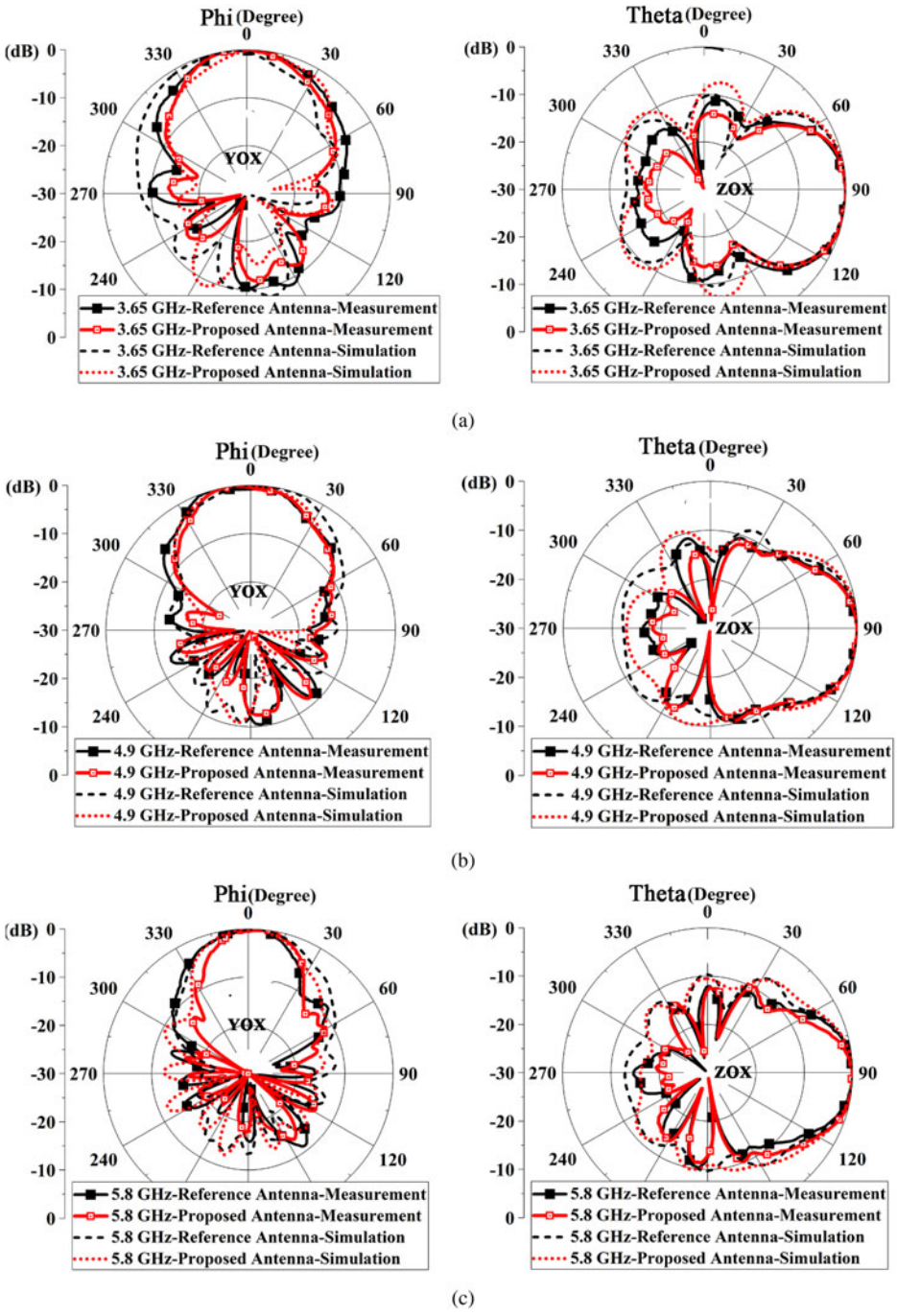

Fig. 8. Measured and simulated radiation patterns (*YOX*-plane and *ZOX*-plane) of reference and proposed antenna array at (a) 3.65 GHz, (b) 4.9 GHz, and (c) 5.8 GHz.

On the other side of the substrate there is a microstrip line ending in a broadband radial quarter-wave stub. In this work, two microstrip-fed Vivaldi antenna arrays have designed to operate at 3.65 and 4.9 and 5.8 GHz printed on an FR4 substrate ($\varepsilon_r = 4.4$, loss tangent = 0.025); it is referred to as the reference antenna whose details are shown in Fig. 4. In the proposed antenna array, 4×14 unit cells are loaded between two antennas, which in Fig. 5, the surface current distribution is shown in two states suggesting that the suppression of surface waves has been done at three operation band wells. The simulated *S*-parameters for the reference and proposed antenna arrays are depicted in Fig. 6. The antennas resonate at 3.65, 4.9, and 5.8 GHz. From the transmission coefficient S_{21}, we see a high reduction in mutual coupling when CTBG-CSRR is located between the radiating elements. The mutual-coupling reduction is 8.5, 10.5, and 18 dB at 3.65, 4.9, and 5.8 GHz, respectively.

Antenna fabrication and measurement

Figure 7 demonstrates a photograph of the fabricated antenna and its measured *S*-parameters. The measured results show excellent agreement with the simulated results. Figure 8 displays the simulated and measurement radiation patterns of the reference and proposed antenna, at 3.65, 4.9, and 5.8 GHz in the *YOX*-plane

https://doi.org/10.1017/S1759078720000215 Published online by Cambridge University Press

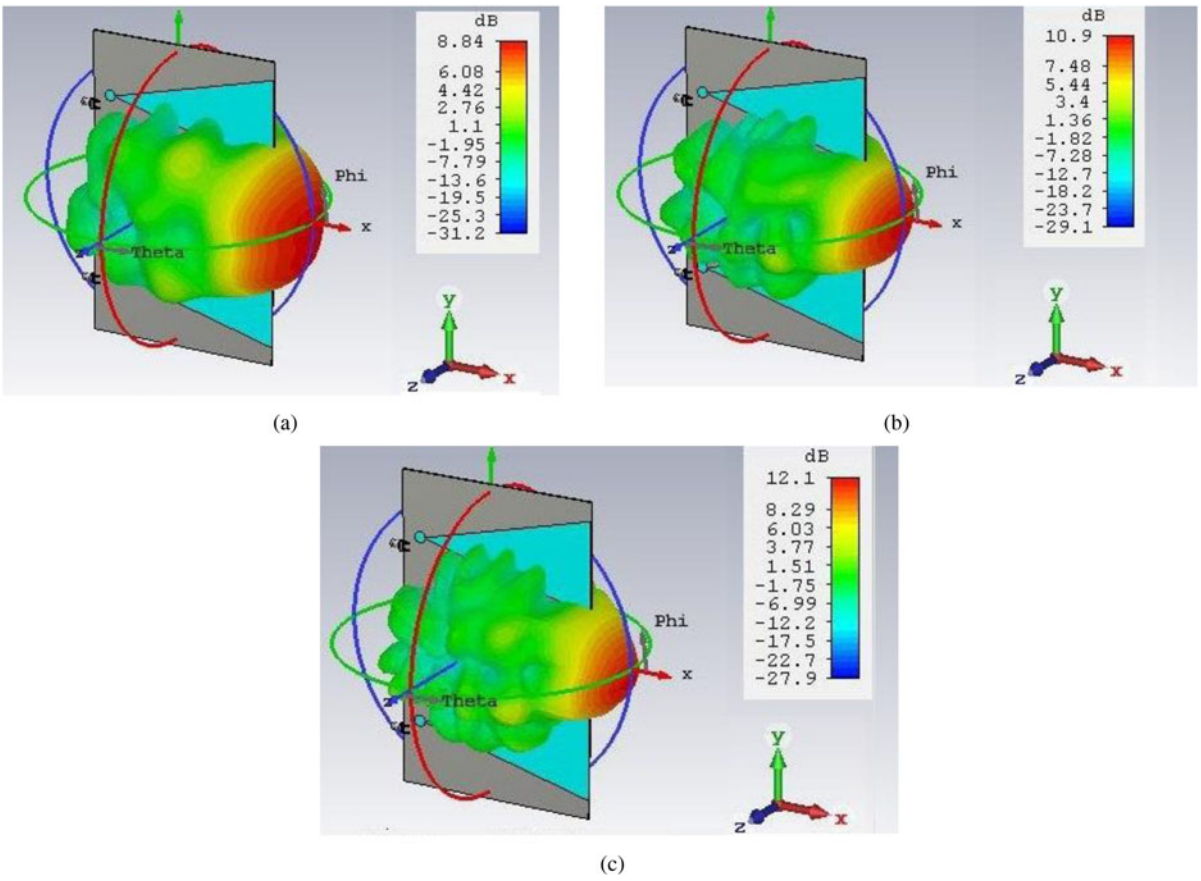

Fig. 9. 3D radiation pattern at (a) 3.65 GHz, (b) 4.9 GHz, and (c) 5.8 GHz.

and the *ZOX*-plane. As can be seen, both radiation antenna parameters are better in three bandgaps which are mentioned in the previous section. Removal of annoying surface waves by CTBG-CSRRs helps improve the antenna radiation performance of maximum gain and front-to-back ratio. Also, in order to have a better image of radiation pattern, the 3D-view of the radiation pattern is presented in Fig. 9. Figure 10 shows the measured and simulated realized gains of the proposed antenna array. The simulated and measurement gain of the traditional antenna array is also included for comparison. The performance of the array for MIMO systems could be checked by the envelope correlation coefficient (ECC). The rich diversity performance with a low correlation coefficient could be achieved. For a two-element antenna system, ECC can be calculated using equation (1) where S_{11} and S_{22} are return losses at two ports, and S_{21} and S_{12} are the isolation parameters [23]:

$$\rho_{12} = \frac{|S_{11}^* S_{12} + S_{21}^* S_{22}|^2}{(1 - |S_{11}|^2 - |S_{21}|^2)(1 - |S_{22}|^2 - |S_{12}|^2)} \quad (1)$$

The ECC has been calculated and compared in Table 1. By reducing the ECC, the higher diversity gain can be ensured.

In Table 1, the performances of the proposed decoupling structures and previous studies are compared from different perspectives such as edge to edge distance, number of operating frequencies, ECC, etc.

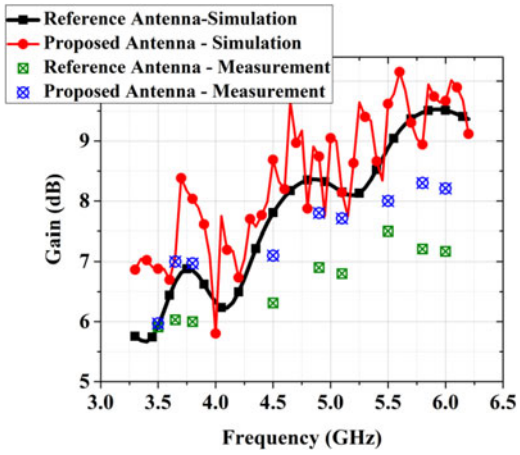

Fig. 10. Comparison of simulated and measured results for the realized gain.

Conclusion

This work presented a CTBG-CSRR unit cell, which is loaded between two microstrip-fed Vivaldi antenna arrays. The final design offered an improvement in decoupling by 8.5, 10.5, and 18 dB at 3.65, 4.9, and 5.8 GHz compared with the reference antenna. The simulated results are validated by measuring manufactured prototypes. The method presented in this paper helped us to achieve an ideal MIMO antenna for WLAN.

https://doi.org/10.1017/S1759078720000215 Published online by Cambridge University Press

Table 1. Performance of the proposed decoupling structures and previous studies

	Reference antenna	Proposed antenna	[17]	[3]	[15]
Operating frequency, f_0 (GHz)	3.65	3.65	5.8	3.3	3.48
	4.9	4.9			4.88
	5.8	5.8			
Edge to edge distance (λ_0)	0.38	0.38	0.14	0.12	0.46
	0.51	0.51			0.65
	0.61	0.61			
Isolation improvement at f_0 (dB)	–	8.5	11–19	55	25.6
	–	10.5			43.7
	–	18			
Gain at f_0 (dB)	6	7	N.M.	8.2	N.M.
	6.9	7.8			
	7.25	8.3			
Antenna bandwidth (%)	75	75	5	3	5 4
Isolation technique	–	CSRR	UC-EBG	Superstrate	Split-EBG
Design and fabrication difficulty	–	Simple	Simple	Difficult	Medium
ECC (dB)	−84 −110 −107	−93 −140 −147	N.M.	−70	−19 −30

N.M., not mentioned.

References

1. **Niakan N** (2014) Mutual Coupling Reduction between Closely Spaced U-slot Patch Antennas by Optimizing Array Configuration and its Applications in MIMO Committee: University of Kansas.
2. **Li J *et al.*** (2019) Dual-band eight-antenna array design for MIMO applications in 5G mobile terminals. *IEEE Access* **7**, 71636–71644.
3. **Jafargholi A, Jafargholi A and Choi JH** (2019) Mutual coupling reduction in an array of patch antennas using CLL metamaterial superstrate for MIMO applications. *IEEE Transactions on Antennas and Propagation* **67**, 179–189.
4. **Yang F and Rahmat-Samii Y** (2003) Microstrip antennas integrated with electromagnetic band-gap (EBG) structures: a low mutual coupling design for array applications. *IEEE Transactions on Antennas and Propagation* **51**, 2936–2946.
5. **Abdalla M, Mahrous A, Mitkees A and Ali A** (2018) Surface wave and mutual coupling reduction between four element linear MIMO array antenna. *International Conference on Aerospace Sciences and Aviation Technology* **15**, 1–6.
6. **Abedin MF and Ali M** (2005) Effects of a smaller unit cell planar EBG structure on the mutual coupling of a printed dipole array. *IEEE Antennas and Wireless Propagation Letters* **4**, 274–276.
7. **Rajo-Iglesias E, Quevedo-Teruel Ó and Inclán-Sánchez L** (2008) Mutual coupling reduction in patch antenna arrays by using a planar EBG structure and a multilayer dielectric substrate. *IEEE Transactions on Antennas and Propagation* **56**, 1648–1655.
8. **Lin B-Q, Liang J, Zeng Y-S and Zhang H-M** (2008) A novel compact and wide-band uni-planar EBG structure. *Progress in Electromagnetics Research* **1**, 37–43.
9. **Coulombe M, Farzaneh Koodiani S and Caloz C** (2010) Compact elongated mushroom (EM)-EBG structure for enhancement of patch antenna array performances. *IEEE Transactions on Antennas and Propagation* **58**, 1076–1086.
10. **Qamar Z, Naeem U, Khan SA, Chongcheawchamnan M and Shafique MF** (2016) Mutual coupling reduction for high-performance densely packed patch antenna arrays on finite substrate. *IEEE Transactions on Antennas and Propagation* **64**, 1653–1660.
11. **Yang XM, Liu XG, Zhou XY and Cui TJ** (2012) Reduction of mutual coupling between closely packed patch antennas using waveguided metamaterials. *IEEE Antennas and Wireless Propagation Letters* **11**, 389–391.
12. **Lee JY, Kim SH and Jang JH** (2015) Reduction of mutual coupling in planar multiple antenna by using 1-D EBG and SRR structures. *IEEE Transactions on Antennas and Propagation* **63**, 4194–4198.
13. **Hafezifard R, Naser-Moghadasi M, Mohassel JR and Sadeghzadeh RA** (2016) Mutual coupling reduction for two closely spaced meander line antennas using metamaterial substrate. *IEEE Antennas and Wireless Propagation Letters* **15**, 40–43.
14. **Iqbal A, Saraereh OA, Bouazizi A and Basir A** (2018) Metamaterial-based highly isolated MIMO antenna for portable wireless applications. *Electronics* **7**, 267.
15. **Tan X, Wang W, Wu Y, Liu Y and Kishk AA** (2019) Enhancing isolation in dual-band meander-line multiple antenna by employing split EBG structure. *IEEE Transactions on Antennas and Propagation* **67**, 2769–2774.
16. **Assimonis SD, Yioultsis TV and Antonopoulos CS** (2012) Computational investigation and design of planar EBG structures for coupling reduction in antenna applications. *IEEE Transactions on Magnetics* **48**, 771–774.
17. **Kumar N and Kiran Kommuri U** (2018) MIMO antenna mutual coupling reduction for WLAN using Spiro Meander line UC-EBG. *Progress in Electromagnetics Research C* **80**, 65–77.
18. **Yu K, Li Y and Liu X** (2018) Mutual coupling reduction of a MIMO antenna array using 3-D novel meta-material structures. *Applied Computational Electromagnetics Society Journal* **33**, 758–763.

https://doi.org/10.1017/S1759078720000215 Published online by Cambridge University Press

19. **Jiao T, Jiang T and Li Y** (2018) A low mutual coupling MIMO antenna using 3-D electromagnetic isolation wall structures. *2017 IEEE 6th Asia-Pacific Conference on Antennas Propagation, APCAP 2017*: Proceeding, vol. 33, no. 3, pp. 1–2.
20. **Luo S, Li Y, Xia Y and Zhang L** (2019) A low mutual coupling antenna array with gain enhancement using metamaterial loading and neutralization line structure. *Applied Computational Electromagnetics Society Journal* **34**, 411–418.
21. **Liu F, Guo J, Zhao L, Huang G-L, Li Y and Yin Y** (2019) Dual-band metasurface-based decoupling method for two closely packed dual-band antennas. *IEEE Transactions on Antennas and Propagation* **68**, 552–557.
22. **Bait-Suwailam MM, Siddiqui OF and Ramahi OM** (2010) Mutual coupling reduction between microstrip patch antennas using slotted-complementary split-ring resonators. *IEEE Antennas and Wireless Propagation Letters* **9**, 876–878.
23. **Chouhan S, Panda DK, Gupta M and Singhal S** (2018) Multiport MIMO antennas with mutual coupling reduction techniques for modern wireless transreceive operations: a review. *International Journal of RF and Microwave Computer-Aided Engineering* **28**, 1–13.

Vahid Najafy received his B.S. degree in electrical engineering from the University of Tabriz, Tabriz, Iran, in 2015 and his M.S. degree from the University of Tarbiat Modares, Tehran, Iran in 2017, His research interests include metamaterial and its applications in antenna engineering.

Mohammad Bemani received his B.S. degree in electrical engineering from the University of KN Toosi University of Technology, Tehran, Iran, in 2007 and his M.S. degree from the University of Tabriz, Tabriz, Iran, in 2009, where he is currently working toward his Ph.D. degree in electrical engineering. His research interests include multi-band and UWB components, reconfigurable antennas, di- electric resonator antennas, and composite right- and left-handed structures.

https://doi.org/10.1017/S1759078720000215 Published online by Cambridge University Press